Distribution of Internal States of CO from O (^{1}D) + CO Determined with Time-Resolved Fourier Transform Spectroscopy

Hui-Fen Chen

Department of Chemistry, National Tsing Hua University, Hsinchu 30013, Taiwan

Yuan-Pern Lee*

Department of Applied Chemistry and Institute of Molecular Science, National Chiao Tung University, Hsinchu 30010, Taiwan, and Institute of Atomic and Molecular Sciences, Academia Sinica, Taipei 10617, Taiwan

Received: June 29, 2006; In Final Form: August 24, 2006

Following collisions of O (^{1}D) with CO, rotationally resolved emission spectra of CO ($1 \le v \le 6$) in the spectral region 1800−2350 cm^{-1} were detected with a step-scan Fourier transform spectrometer. O (^{1}D) was produced by photolysis of O_3 with light from a KrF excimer laser at 248 nm. Upon irradiation of a flowing mixture of O_3 (0.016 Torr) and CO (0.058 Torr), emission of CO ($v \le 6$) increases with time, reaches a maximum ∼10 μs. At the earliest applicable period (2−3 μs), the rotational distribution of CO is not Boltzmann; it may be approximately described with a bimodal distribution corresponding to temperatures ∼8000 and ∼500 K, with the proportion of these two components varying with the vibrational level. A short extrapolation from data in the period 2−6 μs leads to a nascent rotational temperature of ∼10170 ± 600 K for $v = 1$ and ∼1400 ± 40 K for $v = 6$, with an average rotational energy of 33 ± 6 kJ mol^{-1}. Absorption by CO ($v = 0$) in the system interfered with population of low J levels of CO ($v = 1$). The observed vibrational distribution of ($v = 2$):($v = 3$):($v = 4$):($v = 5$):($v = 6$) = 1.00:0.64:0.51:0.32:0.16 corresponds to a vibrational temperature of 6850 ± 750 K. An average vibrational energy of 40 ± 4 kJ mol^{-1} is derived based on the observed population of CO ($2 \le v \le 6$) and estimates of the population of CO ($v = 0$, 1, and 7) by extrapolation. The observed rotational distributions of CO ($1 \le v \le 3$) are consistent with results of previous experiments and trajectory calculations; data for CO ($4 \le v \le 6$) are new.

I. Introduction

The collisional quenching of O (^{1}D) by small molecules is important in the atmospheric heat budget because it transfers the electronic energy to the vibrational energy of these species in the stratosphere.[1,2] The transfer from electronic to vibrational and rotational energy is of interest also for theoretical studies, especially when the process involves a spin-forbidden surface crossing that typically involves a long-lived collisional complex.[3]

The energy transfer of O (^{1}D) to CO has been extensively investigated experimentally[4−13] and theoretically.[14−16] The rate coefficient of quenching for the reaction

$$O(^1D) + CO \rightarrow O(^3P) + CO(v, J) + 190\ \text{kJ mol}^{-1} \quad (1a)$$

was determined to be in the range (5−7) × 10^{-11} cm^3 molecule^{-1} s^{-1}.[4,5,10] The vibrational distribution of CO has been investigated using various methods. Lin and Shortridge probed the absorption of CO, produced from a mixture of O_3, CO, and SF_6 subjected to flash photolysis with a cw CO laser, and reported a vibrational distribution of CO ($v \le 7$) represented by a Boltzmann distribution with a vibrational temperature of ∼5580 K.[8] Their further work yielded a vibrational distribution corresponding to $T \cong 8000$ K and extended the measurements to four temperatures between 246 and 323 K; their observation of nearly equal proportions of C^{16}O and C^{18}O from ^{16}O (^{1}D) + C^{18}O indicates that energy was completely randomized in the CO_2 complex before it dissociated.[9] Harding et al. investigated this process with time-resolved diode laser absorption spectroscopy; they determined the nascent population of CO ($v = 0$) and reported a vibrational population of CO ($0 \le v \le 4$) corresponding to a temperature ∼5000 K.[11] Abe et al. employed vacuum ultraviolet (VUV) laser-induced fluorescence (LIF) to probe the rotational and vibrational distributions of CO produced from reaction 1a.[13] They added ∼2 Torr of Ar to the mixture of O_3 and CO and probed CO at 5 μs after laser irradiation to produce O (^{1}D) so that rotational quenching ensured a Boltzmann rotational distribution at room temperature; the reported vibrational distribution of CO ($v \le 6$) corresponds to a temperature smaller than that reported by Shortridge and Lin.[9] The reported efficiencies for the transfer from electronic to vibrational energy, defined as the ratio of average vibrational energy of CO to the energy of O (^{1}D) relative to O (^{3}P), vary substantially, with values of 17 (ref 13), 21 (ref 6), 25 (ref 11), and 40% (ref 9).

Abe et al. made the only report on the rotational distribution of CO (v); distributions were determined only for vibrational levels $v \le 3$ because of severe overlap of lines of CO ($v \ge 4$) in their LIF spectrum.[13] Rotational distributions of CO ($v = 2$, 3), which can result only from nonadiabatic collisions to form O (^{3}P) + CO (v, J), agree with trajectory calculations performed on a triplet potential-energy surface, whereas those of CO ($v =$

* To whom correspondence should be addressed at the Department of Applied Chemistry and Institute of Molecular Science, National Chiao Tung University. E-mail: yplee@mail.nctu.edu.tw.

10.1021/jp0640676 CCC: $33.50 © 2006 American Chemical Society
Published on Web 10/18/2006

0, 1) show a significant contribution in the low-J levels from the adiabatic process

$$O(^1D) + CO \rightarrow O(^1D) + CO(v \leq 1, J) \qquad (1b)$$

The efficiency for the transfer from electronic to internal (rotational and vibrational) energy was reported to be 29% by Abe et al.[13] and 31% by Matsumi et al.[12]

To understand the dynamics of energy transfer, one must characterize the potential-energy surfaces of the electronic states involved. Only a few theoretical investigations are reported.[17−21] The O (^{1}D) + CO ($X\ ^1\Sigma^+$) channel correlates with an angular CO_2 $^1B_2$ state that lies about 550 kJ mol^{-1} above the ground state. There are three angular states, $^1A_2$, $^3A_2$, and $^3B_2$, with energies less than that of the $^1B_2$ state; all of them cross the $^1B_2$ state. An accurate and balanced calculation of all states involved in the conical intersections remains a demanding task; only the parts near equilibrium geometries of these angular states are characterized.[20]

Experimental investigations on the dynamics of bimolecular reactions or collisional quenching require special attention because these processes need collisions to facilitate reaction, but in the same way collisional quenching of the products might become significant, hence modifying the nascent rotational distribution. In previous work, we have demonstrated that step-scan time-resolved Fourier transform spectroscopy (TR−FTS) is advantageous for studying the dynamics of bimolecular reactions because its multiplex capability allows probing of all states simultaneously, hence assisting understanding the effects of rotational quenching due to collisions.[22,23] Furthermore, TR−FTS has been demonstrated to cover more vibrational−rotational states than resonance-enhanced multiphoton ionization (REMPI) or VUV LIF in detecting HX (X = F, Cl, and Br)[24−29] and CO,[30,31] because REMPI and VUV LIF detection was limited by the short lifetimes of the upper states. We report here an application of time-resolved Fourier transform spectroscopy to investigate the collisional excitation of CO by O (^{1}D) and compare observed distributions of internal states of CO with those from previous reports; information on rotational distributions of CO (v = 4−6) is new.

II. Experiments

The apparatus employed to obtain step-scan time-resolved Fourier transform spectra has been described previously.[26,32,33] The size of the photolysis beam from a KrF laser at 248 nm (Lambda Physik, LPX 200) was ~2.5 × 10 mm^2 at the detection center with a fluence ~200 mJ cm^{-2}. We employed an InSb detector with a rise time of 0.7 μs; its transient signal was preamplified with a factor of 10^5 V A^{-1} (bandwidth 1.5 MHz), followed by further amplification with a factor of 200 (bandwidth 1 MHz) before being digitized with an external data-acquisition board (PAD1232, 12-bit ADC) at 50 ns resolution. Data were typically averaged over 60 laser pulses at each scan step; 7251 scan steps were performed to yield an interferogram resulting in a spectrum of resolution 0.2 cm^{-1} in the spectral region 1800−2350 cm^{-1}. To improve the ratio of signal-to-noise (S/N) of the spectrum, 20 consecutive time-resolved spectra were summed to yield spectra representing emission at intervals 1.0 μs. The temporal response function of the instrument was determined using an IR laser beam as a source, as described previously.[29]

Ozone (O_3) and CO were injected into the reaction chamber with varied partial pressures; to reduce collisional quenching of CO, a minimal pressure was used. For the understanding of the effects of pressure, two sets of data were taken with P_{CO} = 0.058 Torr and P_{O3} = 0.016 Torr, and with P_{CO} = 0.231 Torr and P_{O3} = 0.0686 Torr. A large fraction of O_3 was dissociated upon irradiation at 248 nm based on the reported absorption cross section of 1.5 × 10^{-17} cm^2 molecule^{-1} for O_3 at 248 nm.[34] Flow rates are F_{O_3} = 1.7−2.4 sccm and F_{CO} = 6.3−8.1 sccm; sccm stands for cm^3 per min under standard conditions (273 K and 760 Torr). Depletion of O_3 after each laser pulse is not serious, as was indicated by the negligible change of the signal when we reduced the repetition rate of the photolysis laser from 23 to 12 Hz.

CO (Air Products, 99.9%) was used without purification except for degassing. Ozone was produced from O_2 (Scott Specialty Gases, 99.995%) with an ozone generator (Polymetrics, model T-408), stored over silica gel at 196 K, and eluted from the trap with or without a small flow of He (Scott Specialty Gases, 99.999%). The partial pressure of O_3 was determined by the absorption of Hg emission at 254 nm in a cell with length of 7.0 cm; the absorption cross section of O_3 at 254 nm was taken to be 1.15 × 10^{-17} cm^2.[35]

III. Results and Discussion

Collisional quenching of CO plays an important role in this system. Vibrational quenching of CO by itself or O_3 is relatively slow:

$$CO(v) + CO(v = 0) \rightarrow CO(v - 1) + CO(v = 1) \quad (2)$$

$$CO(v = 1) + O_3(000) \rightarrow CO(v = 0) + O_3(101) \quad (3)$$

with k_2 in the range (3−20) × 10^{-13} cm^3 molecule^{-1} s^{-1} for v = 2 to 7,[11,36,37] and k_3 = 2.0 × 10^{-12} cm^3 molecule^{-1} s^{-1}.[11] With both [CO] and [O_3] less than 5 × 10^{15} molecules cm^{-3} (~0.15 Torr at 298 K), vibrational quenching of CO is less than 10% of the original population within 10 μs. Rotational quenching is, however, much more rapid and must be taken into account. To maintain a nearly collisionless condition within a 3.0 μs period, the pressures of the system were made as small as practicable while maintaining a satisfactory signal-to-noise ratio.

Figure 1 shows emission spectra of CO at a resolution of 0.2 cm^{-1}, recorded 1.0−2.0, 2.0−3.0, 5.0−6.0, 9.0−10.0, and 22−23 μs after photolysis of a flowing mixture of O_3 and CO with partial pressures of 0.016 and 0.058 Torr, respectively; eight spectra recorded under similar conditions were averaged to improve the ratio of signal-to-noise. The smaller intensity in periods 1.0−3.0 μs reflects the small rate of production of internally excited CO; the signal attains a maximum near 10 μs, followed by a slow decay. For comparison, Figure 2 shows emission spectra of CO recorded 1.0−2.0, 2.0−3.0, 6.0−7.0, and 10−11 μs after 248 nm photolysis of a flowing mixture of O_3 and CO with partial pressures of 0.0686 and 0.231 Torr, respectively. Rotational quenching is more severe in these spectra relative to those at low pressure. Hence, we chose the period 2−3 μs in Figure 1 as a representative spectrum for analysis; under these conditions the ratio of signal-to-noise is satisfactory for quantitative analysis while the rotational quenching is still small.

An expanded partial spectrum of Figure 1B is shown in Figure 3. Assignments based on spectral parameters reported by Ogilvie et al.[38] are shown as stick diagrams; values of J' are indicated. The spectrum indicates that the 0.2 cm^{-1} resolution is adequate to resolve a large number of lines involving v = 1−6. The emission spectra in Figure 1 exhibit emission of CO with J' up to 68 and v' up to 6.

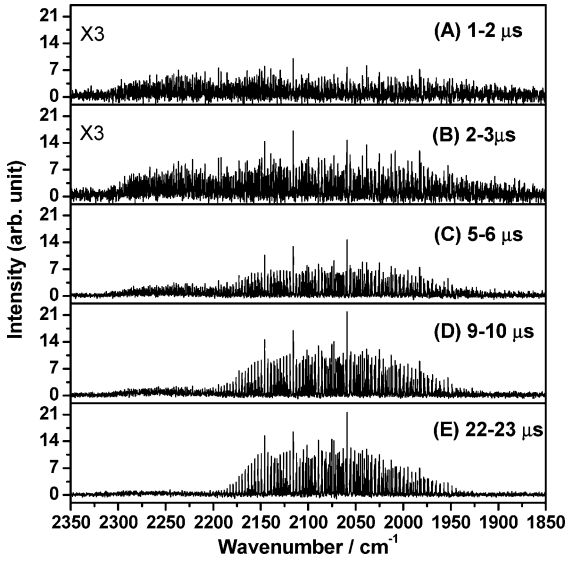

Figure 1. Infrared emission spectra of CO in spectral region 1850−2350 cm^{-1} recorded at varied intervals upon photolysis of a flowing mixture of O_3 (0.016 Torr) and CO (0.058 Torr) at 248 nm. (A) 1.0−2.0 μs; (B) 2.0−3.0 μs; (C) 5.0−6.0 μs; (D) 9.0−10.0 μs; (E) 22−23 μs. Spectral resolution is 0.2 cm^{-1}; 60 laser pulses were averaged at each scan step of the interferometer. Eight spectra recorded under similar conditions were averaged.

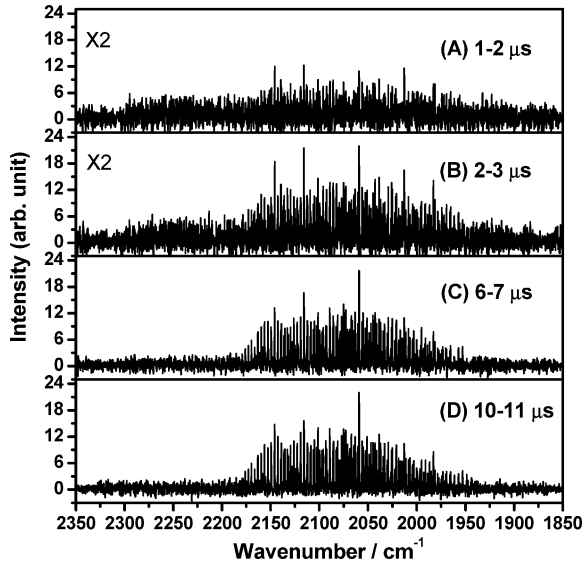

Figure 2. Infrared emission spectra of CO in spectral region 1850−2350 cm^{-1} recorded at varied intervals upon photolysis of a flowing mixture of O_3 (0.0686 Torr) and CO (0.231 Torr) at 248 nm. (A) 1.0−2.0 μs; (B) 2.0−3.0 μs; (C) 6.0−7.0 μs; (D) 10.0−11.0 μs. Spectral resolution is 0.2 cm^{-1}; 60 laser pulses were averaged at each scan step of the interferometer.

1. Rotational Distribution of CO. We calculated values of the Einstein A coefficient according to this formula,[30]

$$A_{\upsilon J}^{\upsilon' J'} = \frac{16\pi^3\tilde{\nu}^3|\iota||\langle\upsilon'|p(R)|\upsilon\rangle|^2(1 + C_\upsilon^{\upsilon'}\iota + D_\upsilon^{\upsilon'}\iota^2)}{3\epsilon_0 h(2J' + 1)} \quad (4)$$

in which $\tilde{\nu}$ is the wavenumber of a transition from a vibration−rotational state (υ', J') to another state (υ'', J''), $\iota = {}^1/_2[J'(J' + 1) - J''(J'' + 1)]$ is a running number depending on rotational quantum numbers J' and J'', $\langle\upsilon'|p(R)|\upsilon''\rangle$ is a pure vibrational matrix element of electric dipolar moment between vibrational states υ' and υ'', $C_\upsilon^{\upsilon'}$ and $D_\upsilon^{\upsilon'}$ are coefficients in the Herman−Wallis factor to take into account the rotational effect on the vibrational matrix element,[39] and ϵ_0 and h are fundamental constants. Each vibration−rotational line was normalized with the instrument response function, and divided by its respective Einstein coefficient to yield a relative population $P_\upsilon(J')$. Partially overlapped lines, such as $J' = 22$, 29, 39 of CO ($\upsilon' = 1$), $J' = 7$, 19, 22, 35 of CO ($\upsilon' = 2$), $J' = 6$, 15, 24, 32 of CO ($\upsilon' = 3$), and $J' = 2$, 14, 26 of CO ($\upsilon' = 4$), were deconvoluted to yield their intensities.

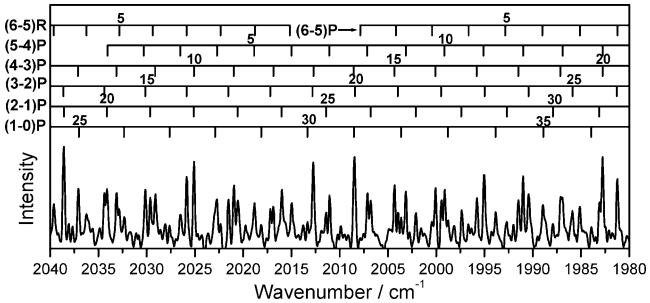

Figure 3. Expanded view of partial infrared emission spectra of CO in Figure 1B, 2.0−3.0 μs. Assignments are shown in stick diagrams.

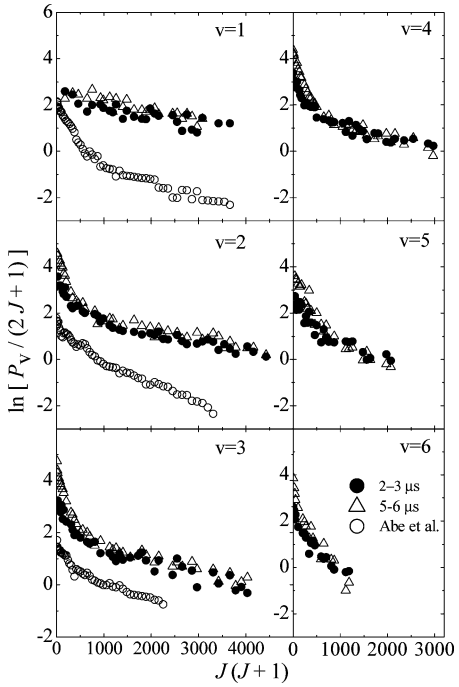

Figure 4. Semilogarithmic plots of relative rotational populations of CO ($\upsilon = 1-6$) upon photolysis of a flowing mixture of O_3 (0.016 Torr) and CO (0.058 Torr) at 248 nm. Results of Abe et al.,[13] displaced vertically downward by two units for clarity, are also shown as ○.

Semilogarithmic plots of $P_\upsilon(J')/(2J' + 1)$ vs $J'(J' + 1)$ for CO ($\upsilon = 1-6$) produced from O (^{1}D) + CO at 2−3 μs (marked ●) and 5−6 μs (marked Δ) are shown in Figure 4. These figures provide information on the extent of rotational quenching; quenching before 6 μs is present but not serious, it affects slightly the low-J distribution and requires only a small correction. For the period of 2−3 μs, rotational distributions are not Boltzmann for CO ($\upsilon = 2-5$), whereas those of CO ($\upsilon = 1$) and CO ($\upsilon = 6$) may be fitted with a Boltzmann distribution having rotational temperatures 8380 ± 1240 K and 1120 ± 100 K, respectively; unless specified, error limits listed in this paper represent one standard deviation in fitting. Rotational distributions of CO ($\upsilon = 1-3$) reported by Abe et al.[13] (symbol ○, displaced vertically downward for clarity) are shown also in Figure 4 for comparison. For CO ($\upsilon = 3$), their results agree with ours satisfactorily except that our experiments

TABLE 1: Fitted Rotational Temperature, Rotational Energy, and Vibrational Population of CO (v) Recorded 2.0−3.0 μs after Irradiation of a Flowing Mixture of O_3 (0.016 Torr) and CO (0.058 Torr) at 248 nm

v	T_r/K		$E_r(v)$/kJ mol^{-1}	vibr population
0				(0.372)[d]
1		8380 ± 1240 [10170 ± 610][b]	36.3	0.977[c] (0.236)
2	610 ± 70[a]	7930 ± 540 [8800 ± 260]	28.1	1.000 (0.142)
3	580 ± 40	5870 ± 640 [7530 ± 490]	23.9	0.642 (0.091)
4	530 ± 50	5280 ± 670 [6610 ± 250]	21.6	0.510 (0.073)
5	500 ± 90	4450 ± 2000 [6290 ± 260]	13.5	0.322 (0.046)
6		1120 ± 100 [1490 ± 30]	7.6	0.162 (0.023)
	(390 ± 30)[e]	(3390 ± 460)[e]		
7				(0.017)
av			26.3 ± 3.6	

[a] Low-J component of the bimodal distribution. [b] Rotational temperature extrapolated to $t = 0$; only high-J component was considered for $v = 2-5$. [c] Observed population relative to that of $v = 2$; see text. [d] Normalized population with $v = 0$, 1, and $v = 7$ predicted from Boltzmann distribution; see text. [e] Estimated by assuming a temperature of 3390 K for the high-J component; see text.

extend observed J' to much larger values. In contrast, the distribution of CO ($v = 1$) reported by Abe et al. shows a much greater population for $J \leq 20$ than ours. Rotational distributions of CO ($v = 4-6$) in this work are new. Although Abe et al. observed these vibrational levels, severe overlap of lines associated with these levels prevented them from undertaking further rotational analysis.

In our experiment, absorption of CO ($v = 0$) in the system might interfere with measurements of the emission of CO ($v = 1$) because the emission was collected with a multipass Welsh cell. For example, with a reported infrared absorption cross section of 5.4×10^{-17} cm^2 for the R line of CO ($v'' = 0$, $J'' = 5$),[40] an estimated absorption length of 80 cm, a concentration of [CO] = 2.08×10^{15} molecules cm^{-3}, and a fraction of 8% of the total population for this level of CO at 298 K, a transmission of ~50% is estimated. Hence, the population of the low-J component of CO ($v = 1$) determined in this work is unreliable and is not used. Correction for this absorption involves large uncertainties and is not recommended.

For convenience of description we fitted the rotational distributions of CO ($v = 2-5$) with a double Boltzmann distribution function to derive the rotational temperature of high-J and low-J components. Results for $t = 2.0-3.0$ μs are listed in Table 1. For the high-J component, the rotational temperature decreases with vibrational excitation. There is likely also an unresolved high-J component in the observed distribution of CO ($v = 6$) that overlaps with the low-J component. If we employed an estimated rotational temperature of 3400 K for the high-J component, we derived a rotational temperature of 390 ± 30 K for the low-J component, consistent with the decreasing trend.

Rotational temperatures of CO ($v = 1$), CO ($v = 6$), and the high-J components of CO ($2 \leq v \leq 5$) as a function of reaction period are shown in Figure 5. With a short extrapolation, we estimate the nascent rotational temperature to be 10170 ± 610, 8800 ± 260, 7530 ± 490, 6610 ± 250, 6290 ± 260, and 1490 ± 30 K for CO ($v = 1$) to CO ($v = 6$), respectively, as listed in Table 1. The correction factors for rotational temperature at 2−3 μs to derive nascent rotational temperature, taken as ratios

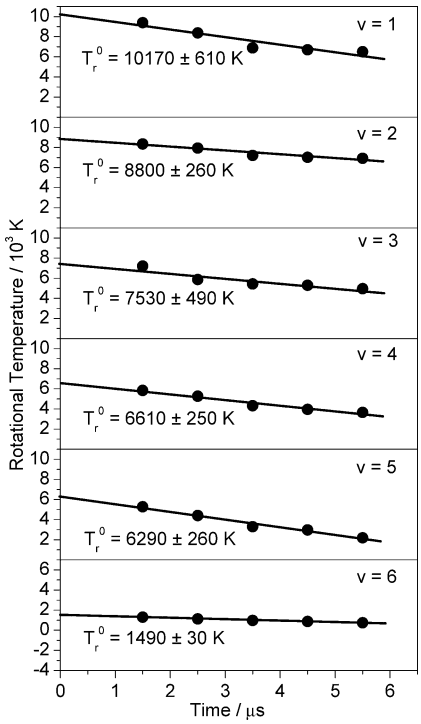

Figure 5. Rotational temperature of CO ($v = 1-6$) as a function of time.

of extrapolated nascent temperature to observed rotational temperature at 2−3 μs, are thus 1.21, 1.11, 1.28, 1.25, 1.41, and 1.33 for CO ($v = 1$) to CO ($v = 6$), respectively, and with an average of 1.26 ± 0.10. In contrast, the rotational temperature for CO ($v = 1$) and CO ($v = 6$) in the period 1.0−3.0 μs under high pressure (shown in Figure 2) are 870 ± 120 K and 570 ± 150 K, respectively, indicating severe quenching under such conditions.

Rotational energies for each vibrational level, $E_r(v)$, obtained on summing a product of rotational energy and normalized population for each rotational level, are listed in Table 1. An average rotational energy $E_r = 26 \pm 4$ kJ mol^{-1} for CO ($v = 1-6$) observed 2.0−3.0 μs after photolysis is derived on summing a product of vibrational population and associated $E_r(v)$; the vibrational population is discussed in the next section. After applying a correction factor 1.26 ± 0.10 for rotational quenching, we derive a nascent rotational energy of 33 ± 6 kJ mol^{-1} based on observed data.

2. Vibrational Distribution of CO. Relative populations obtained on counting levels up to observed J_{max} in each vibrational level are indicated as $\sum_J P_v(J)$. For $v = 1$, we used extrapolated values for $J \leq 20$ by assuming a Boltzmann distribution. We normalized values of $\sum_J P_v(J)$ derived from the spectrum in Figure 1B for each vibrational state to yield a ratio of vibrational populations ($v = 1$):($v = 2$):($v = 3$):($v = 4$):($v = 5$):($v = 6$) = 0.98:1.00:0.64:0.51:0.32:0.16. This distribution is plotted in Figure 6 and compared with that from previous reports. Because of possible errors in deriving the population of CO ($v = 1$), we represent vibrational populations of CO (v) relative to that of CO ($v = 2$). The distribution of CO ($v = 2-6$) corresponds to a vibrational temperature of 6850 ± 730 K.

Vibrational distributions reported previously are compared with our results in Figure 6. Our results (symbol ●) for CO ($v \geq 2$) agree with those of Shortridge and Lin (symbol ▽),[9] who reported ($v = 1$):($v = 2$):($v = 3$):($v = 4$):($v = 5$):($v = 6$) = 1.56:1.00:0.75:0.55:0.38:0.19. The distribution reported by

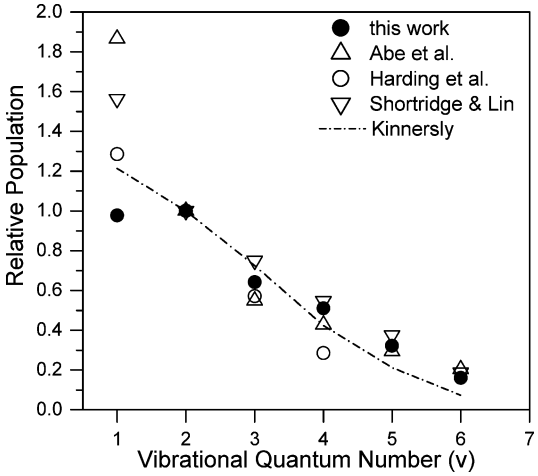

Figure 6. Comparison of relative vibrational distributions of CO from O (^{1}D) + CO. Key: (●) this work; (▽) Shortridge and Lin;[9] (△) Abe et al.;[13] (○) Harding et al.;[11] (dot−dash line) Kinnersly.[15]

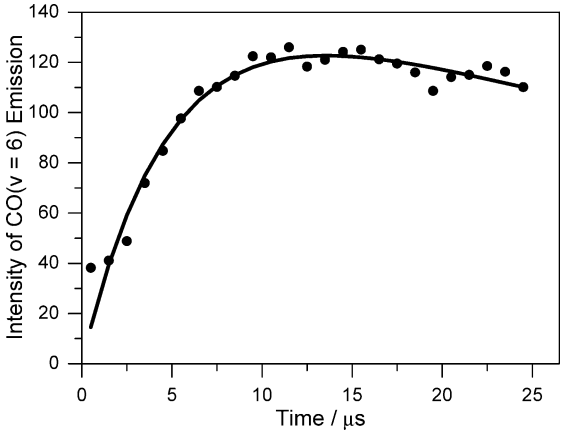

Figure 7. Temporal profiles of CO (v = 6), shown as ●, upon photolysis of a flowing mixture of O_3 (0.016 Torr) and CO (0.058 Torr) at 248 nm. The solid line represents a fitting to a simple rise and decay mechanism.

Harding et al. (symbol ○) [11] with (v = 0):(v = 1):(v = 2):(v = 3):(v = 4) = 4.28:1.29:1.00:0.57:0.29 corresponds to a smaller temperature. The ratio reported by Abe et al. (symbol Δ)[13] with (v = 0):(v = 1):(v = 2):(v = 3):(v = 4):(v = 5):(v = 6) = 4.30:1.87:1.00:0.55:0.43:0.29:0.20 also differs slightly from ours. The vibrational distribution predicted by Kinnersly using a classical collision complex model and potentials previously derived for C(^{3}P) + O_2 ($^3\Sigma_g^-$), agrees satisfactorily also with our observations, as shown with a dot−dash line in Figure 6.

Assuming a Boltzmann vibrational distribution, we estimate the population of v = 0, 1, and 7 relative to v = 2 to be 2.62, 1.66, and 0.12, respectively. The vibrational distribution of CO normalized for v = 0−7 is thus (v = 0):(v = 1):(v = 2):(v = 3):(v = 4):(v = 5):(v = 6):(v = 7) = 0.372:0.236:0.142:0.091:0.073:0.046:0.023:0.017, as shown in Table 1. The average vibrational energy of CO derived from our data is E_v = 40 ± 4 kJ mol^{-1}. Our value is similar to values of 42 ± 3 kJ mol^{-1} reported by Shortridge and Lin[9] and 37 ± 3 kJ mol^{-1} by Abe et al.,[13] but much greater than the value of 21 ± 3 kJ mol^{-1} by Harding et al.[11]

The large extent of vibrational excitation can be rationalized according to a large variation in the bond lengths of the $^3B_2$ state (and other angular states that might be involved) of CO_2 relative to that of the ground state of CO. The bond length of these angular states is predicted to be in the range 1.25−1.26 Å,[20] whereas that of CO was determined to be 1.128 Å.[38]

3. Temporal Profiles of Emission. The total intensity of CO emission was derived by integration of all lines associated with CO in the spectrum. Emission of CO reaches a maximum at ∼10 μs, followed by a slow decay; the data acquisition terminated at 24 μs due to limitations of memory. This temporal profile is nearly identical to that recorded directly with the detector and an oscilloscope because CO is the only emitter. The temporal profile cannot be fitted with a simple function consisting of an exponential rise and an exponential decay because the rise and decay of many different vibrational levels of CO are involved.

The temporal evolution of emission of CO (v = 6), the highest observable vibrational state, upon irradiation of a flowing mixture of O_3 (0.016 Torr) and CO (0.058 Torr) at 248 nm is shown in Figure 7. We deconvoluted this profile with the instrument response function and modeled them with a mechanism consisting of formation and quenching of first order to derive a rate coefficient of formation k_f = (2.0 ± 0.3) × 10^5 s^{-1} and of quenching k_q = (1.7 ± 0.7) × 10^4 s^{-1} for CO. The slow rate of formation is consistent of a mechanism involving a long-lived adduct, as previously proposed. Using [CO] = 1.9 × 10^{15} molecules cm^{-3} and literature values of k_{1a} = (4−7) × 10^{-11} cm^3 molecule^{-1} s^{-1},[4,5,10] we derive a pseudo-first-order rate coefficient k_{1a}^I = (8−13) × 10^4 s^{-1} for reaction 1a, slightly smaller than observed k_f in this work. The rate of quenching for CO (v = 6) due to CO (v = 0) was reported to be ∼8.4 × 10^{-13} cm^3 molecule^{-1} s^{-1},[41,42] corresponding to a pseudo-first-order rate coefficient of 1.7 × 10^3 s^{-1} under our experimental conditions, much smaller than observed k_q. This might indicate that quenching of CO (v = 6) by O_3 is much greater than by CO. The rate of quenching for this process is unreported, but is expected to be greater than k_3 (2.0 × 10^{-12} cm^3 molecule^{-1} s^{-1}), quenching rate of CO (v = 1) by O_3.[11]

4. Comparison of Rotational Distribution with Trajectory Calculations. Abe et al. predicted a rotational distribution of CO from reaction 1 with trajectory calculations.[13] Collisions of O (^{1}D) with CO produce CO_2 in its $^1B_2$ state, which intersects with the $^3B_2$ state of CO_2. All trajectories begin at the seam between the $^1B_2$ and the $^3B_2$ surfaces, which ranges from θ = 100°−130° for the bending angle and R = 1.2−1.5 Å for the bond length of the new C−O bond; the transition probability was assumed to be constant over this seam. The potential-energy surface was calculated with the MP2/6-31G* method and fitted to an extended LEPS function by means of the least-squares method.

Figure 8 compares rotational distributions observed in this work (symbol ●) with those predicted with trajectory calculations (indicated with bars) and observed experimentally (symbol ○) with VUV LIF by Abe et al.;[13] experimental results were scaled to provide an effective overlap between J = 20−50 for CO (v = 2). The agreement for the rotational distribution of CO (v = 2, 3) among both experiments and the calculation is satisfactory, whereas for CO (v = 1) our result agrees with the calculation, but not with the experiment by Abe et al.[13] They attributed the excess population for CO (v = 1, 0 ≤ J ≤ 25) to the adiabatic process, reaction 1b.

With the available kinetic energy, 33 kJ mol^{-1}, of O (^{1}D) from photolysis of O_3 at 248 nm, only v ≤ 1 levels of CO can be populated from the adiabatic process. We are unable to observe the extra population for CO (v = 1, J ≤ 20) as reported by Abe et al.[13] partly because of the absorption by CO (v = 0) and partly because of the kinetic energy of O (^{1}D) might be partially thermalized in our system. The distribution of high-J

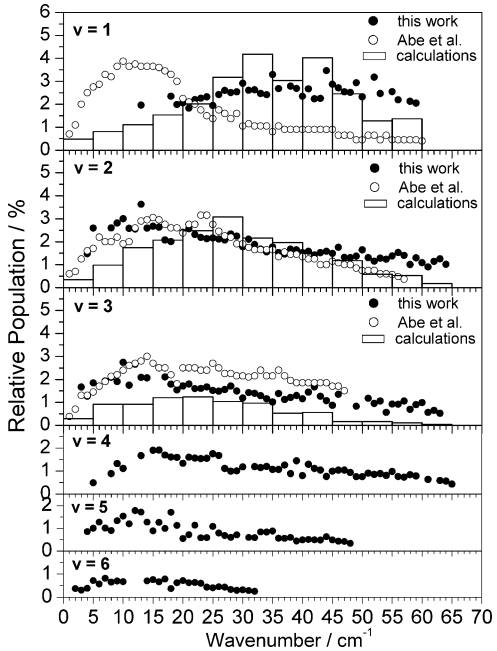

Figure 8. Comparison of rotational populations of CO ($v = 1-6$) from O (^{1}D) + CO. Key: (●) this work; (○) experiments from Abe et al.; (bars) trajectory calculations from Abe et al.[13]

levels of CO ($v = 1$) observed in this work agrees with trajectory calculations much better than that of Abe et al. Similar results of enhanced low-*J* component of CO ($v = 0$) were also reported by Abe et al., but we are unable to probe the population of CO ($v = 0$) with our technique.

Elastic collisions with no exchange of atoms and inelastic collisions with exchange of oxygen atoms were distinguished in the trajectory calculations; the former has more contributions to production of CO ($v = 0$ and 1), whereas the latter has more contributions to production of CO ($v = 2$ and 3).[13] The elastic collisions tend to provide increased rotational excitation. We are unable to distinguish these two processes in this work; isotopic experiments are infeasible in our experiments using rapidly flowing gases. Observed bimodal distribution is consistent with the general picture predicted with previous trajectory calculations: inelastic collisions produce smaller rotational excitation but greater vibrational excitation, whereas the elastic collisions produce greater rotational excitation but smaller vibrational excitation.

Previous trajectory calculations take into account only the $^3B_2$ potential-energy surface. According to quantum-chemical calculations, the $^3A_2$ and $^1A_2$ surfaces might also play a role.[20] The $^1B_2$ state crosses the $^3B_2$ and $^3A_2$ states at distinctly different angles (~92 and 109° at $R = 2.35$ Bohr) and the equilibrium angles for $^3B_2$ and $^3A_2$ states (118.5 and 127.4°) also vary substantially. If CO_2 adduct dissociates via these two states, the rotational distribution of CO might be distinctively different. Our observed non-Boltzmann (bimodal) distribution of CO is also consistent with a model that reaction 1a is associated with two or more dissociation paths. More sophisticated calculations are needed to enhance the understanding of the dynamics of these energy transfer processes and to compare with our experimental results.

5. Comparison of Energy Transfer. Stolow and Lee,[43] and later Lu et al.[44] investigated the photodissociation dynamics of CO_2 at 157 nm using photofragmentation translational spectroscopy; the latter authors employed direct VUV ionization with synchrotron radiation for detection. An average translational energy was estimated to be ~150 kJ mol^{-1} based on their reported distribution of translational energy for the minor channel (~4%)

$$CO_2 + h\nu \rightarrow CO\ (^1\Sigma^+) + O\ (^3P) \qquad (5)$$

Given the excess energy of 230 kJ mol^{-1} for reaction 5 upon 157 nm photodissociation, the internal energy of CO is estimated to be ~80 kJ mol^{-1}. The energy of CO_2 excited with light at 157 nm is only ~10 kJ mol^{-1} greater than the O (^{1}D) + CO system upon photolysis of a mixture of O_3 and CO at 248 nm. The value of 80 kJ mol^{-1} estimated for the internal energy of CO produced from photolysis of CO_2 at 157 nm in the molecular beam is similar to the value that we determined for reaction 1a: 33 ± 6 kJ mol^{-1} for rotation and 40 ± 4 kJ mol^{-1} for vibration.

The efficiency for E−V energy transfer determined in this work is 40/(190) = ~21%; the initial translational energy of O (^{1}D) was not taken into account. This value is similar to values 17% by Abe et al.[13] and 21% reported by Shortridge and Lin,[9] but greater than values 11% derived from the vibrational distribution reported by Harding et al.[11] Harding et al. reported an efficiency of $25 \pm {}_5{}^8$ % based on their measurements of the total number of CO ($v = 1$) produced after collision with O (^{1}D), with the quenching of CO by O_3 taken into account. The efficiency for the transfer of electronic to internal energy determined in this work, 38%, greater than values (29−31%) reported previously by Abe et al.[13] and Matsumi et al.[12]

IV. Conclusion

Rotationally resolved emission of CO up to $v = 6$ and $J = 68$ is observed upon photolysis of a flowing mixture of O_3 and CO at 248 nm; internally excited CO is produced via collisions of O (^{1}D) and CO. The average rotational energy of 33 ± 6 kJ mol^{-1} and vibrational energy of 40 ± 4 kJ mol^{-1} for CO indicate that a substantial fraction of available energy is partitioned into the internal energy of CO, with $f_r \cong 0.17 \pm 0.03$ and $f_v \cong 0.21 \pm 0.02$. Rotational distributions of CO ($v = 2$, 3) agree with previous experiments and trajectory calculations by Abe et al.[13] Rotational distributions of CO ($v = 4-6$) are new; they exhibit less rotational excitation than those in CO ($v = 1-3$).

Acknowledgment. The National Science Council of Taiwan supported this work under Contract No. NSC95-2119-M-009-032.

References and Notes

(1) Taylor, R. L. *Can. J. Chem.* **1974**, *52*, 1436.
(2) Harris, R. D.; Adams, G. W. *J. Geophys. Res.* **1983**, *88*, 4918.
(3) Lemont, S.; Flynn, G. W. *Annu. Rev. Phys. Chem.* **1977**, *28*, 261.
(4) Collins, R. J.; Hussain, D. *J. Photochem.* **1973**, *1*, 481.
(5) Slanger, T. G.; Black, G. *J. Chem. Phys.* **1968**, *49*, 4758.
(6) Slanger, T. G.; Black, G. *J. Chem. Phys.* **1974**, *60*, 468.
(7) Lin, M. C.; Bauer, S. H. *J. Chem. Phys.* **1969**, *50*, 3377.
(8) Lin, M. C.; Shortridge, R. G. *Chem. Phys. Lett.* **1974**, *29*, 42.
(9) Shortridge, R. G.; Lin, M. C. *J. Chem. Phys.* **1976**, *64*, 4076.
(10) Davidson, J. A.; Schiff, H. I.; Brown, T. J.; Howard, C. J. *J. Chem. Phys.* **1978**, *69*, 1216.
(11) Harding, D. R.; Weston, R. E., Jr.; Flynn, G. W. *J. Chem. Phys.* **1989**, *88*, 3590.
(12) Matsumi, Y.; Inagaki, Y.; Morley, G. P.; Kawasaki, M. *J. Chem. Phys.* **1994**, *100*, 315.
(13) Abe, M.; Inagaki, Y.; Springsteen, L. L.; Matsumi, Y.; Kawasaki, M.; Tachikawa, H. *J. Phys. Chem.* **1994**, *98*, 12641.
(14) Tully, J. C. *J. Chem. Phys.* **1975**, *62*, 1893.
(15) Kinnersly, S. R. *Mol. Phys.* **1979**, *38*, 1067.
(16) Zahr, G. E.; Preston, R. K.; Miller, W. H. *J. Chem. Phys.* **1975**, *62*, 1127.

(17) Julienne, P. S.; Neuman, D.; Kraus, M. *J. Atmos. Sci.* **1971**, *28*, 833.
(18) Englebrecht, L.; Liu, B. *J. Chem. Phys.* **1983**, *78*, 3097.
(19) Simkin, V. Y.; Dementev, A. I.; Pupyshev, V. I. *Russ. J. Phys. Chem.* **1982**, *56*, 1739.
(20) Spielfield, A.; Feautrier, N.; Cossart-Magos, C.; Chambaud, G.; Rosmus, P.; Werner, H.-J.; Botschwina, P. *J. Chem. Phys.* **1992**, *97*, 8382.
(21) Buenker, R. J.; Honigmann, M.; Liebermann, H.-P.; Kimura, M. *J. Chem. Phys.* **2000**, *113*, 1046.
(22) Chen, K.-S.; Cheng, S.-S.; Lee, Y.-P. *J. Chem. Phys.* **2003**, *119*, 4229.
(23) Cheng, S.-S.; Wu, Y.-J.; Lee, Y.-P. *J. Chem. Phys.* **2004**, *120*, 1792.
(24) Lin, S.-R.; Lin, S.-C.; Lee, Y.-C.; Chou, Y.-C.; Chen, I.-C.; Lee, Y.-P. *J. Chem. Phys.* **2001**, *114*, 160.
(25) Lin, S.-R.; Lin, S.-C.; Lee, Y.-C.; Chou, Y.-C.; Chen, I.-C.; Lee, Y.-P. *J. Chem. Phys.* **2001**, *114*, 7396.
(26) Wu, C.-Y.; Chung, C.-Y.; Lee, Y.-C.; Lee, Y.-P. *J. Chem. Phys.* **2002**, *117*, 9785.
(27) Wu, C.-Y.; Wu, Y.-J.; Lee, Y.-P. *J. Chem. Phys.* **2004**, *121*, 8792.
(28) Bahou, M.; Lee, Y.-P. *Aus. J. Chem.* **2004**, *57*, 1161.
(29) Yang, S.-K.; Liu, S.-Y.; Chen, H.-F.; Lee, Y.-P. *J. Chem. Phys.* **2005**, *123*, 224304.
(30) Wu, C.-Y.; Lee, Y.-P.; Ogilvie, J. F.; Wang, N. S. *J. Phys. Chem. A*, **2003**, **107**, 2389.
(31) Wu, C.-Y.; Lee, Y.-P.; Wang, N. S. *J. Chem. Phys.* **2004**, *120*, 6957.
(32) Yeh, P.-S.; Leu, G.-H.; Lee, Y.-P.; Chen, I.-C. *J. Chem. Phys.* **1995**, *103*, 4879.
(33) Lin, S.-R.; Lee, Y.-P. *J. Chem. Phys.* **1999**, *111*, 9233.
(34) Matsumi, Y.; Kawasaki, M. *Chem. Rev.* **2003**, *103*, 4767.
(35) DeMore, W. B.; Raper, O. *J. Phys. Chem.* **1964**, *68*, 412.
(36) Powell, H. T. *J. Chem. Phys.* **1973**, *59*, 4937.
(37) Liu, Y. S.; McFarlane, R. A.; Wolga, G. J. *J. Chem. Phys.* **1975**, *63*, 228.
(38) Ogilvie, J. F.; Cheah, S.-L.; Lee, Y.-P.; Sauer, S. P. A. *Theor. Chem. Acc.* 2002**,** *85*, 108.
(39) Ogilvie, J. F. *The Vibrational and Rotational Spectrometry of Diatomic Molecules*; Academic Press: London, 1998.
(40) Rothman, L. S.; Rinsland, C. P.; Goldman, A.; Massie, S. T.; Edwards, D. P.; Flaud, J.-M.; Perrin, A.; Camy-Peyret, C.; Dana, V.; Mandin, J.-Y.; Schroeder, J.; McCann, A.; Gamache, R. R.; Wattson, R. B.; Yoshino, K.; Chance, K. V.; Jucks, K. W.; Brown, L. R.; Nemtchinov, V.; Varanasi, P. *J. Quant. Spectrosc. Radiat. Transfer* **1998**, *60*, 665.
(41) Powell, H. T. *J. Chem. Phys.* **1973**, *59*, 4937.
(42) Liu, Y. S.; McFarlane, R. A.; Wolga, G. J. *J. Chem. Phys.* **1975**, *63*, 228.
(43) Stolow, A.; Lee, Y.-T. *J. Chem. Phys.* **1993**, *98*, 2066.
(44) Lu, I.-C.; Lin, J. J.; Lee, S.-H.; Lee, Y.-T.; Yang, X.-M. *Chem. Phys. Lett.* **2003**, *382*, 665.